POLITECNICO DI TORINO
Repository ISTITUZIONALE

Moment-Based Constrained Optimal Control of Wave Energy Converters: Flap-Type Device

Original
Moment-Based Constrained Optimal Control of Wave Energy Converters: Flap-Type Device / Faedo, N., Ringwood, J.V.. - 51:(2018), pp. 50-55. (11th IFAC Conference on Control Applications in Marine Systems, Robotics, and Vehicles (CAMS)) [10.1016/j.ifacol.2018.09.468].

Availability:
This version is available at: 11583/2988074 since: 2024-04-24T12:17:01Z

Publisher:
ELSEVIER

Published
DOI:10.1016/j.ifacol.2018.09.468

Terms of use:

This article is made available under terms and conditions as specified in the corresponding bibliographic description in the repository

Publisher copyright

(Article begins on next page)

26 June 2026

Available online at www.sciencedirect.com

ScienceDirect

IFAC PapersOnline CONFERENCE PAPER ARCHIVE

IFAC PapersOnLine 51-29 (2018) 50–55

Moment-Based Constrained Optimal Control of Wave Energy Converters: Flap-Type Device ⋆

Nicolás Faedo * **John V. Ringwood** *

* *Centre for Ocean Energy Research, Maynooth University, Maynooth, Ireland (e-mail: nicolas.faedo@mu.ie).*

AbstractThe control objective for Wave Energy Converters (WECs) deviates significantly from the traditional reference "tracking" problem. In fact, a suitable control formulation for WECs should *optimise the energy absorption from waves* while observing, at the same time, the physical limitations of both the device and the actuator. Due to the irregular motion of the sea, computing an optimal control law achieving such objectives is non-trivial. This paper presents the application of a recently developed moment-based optimal control strategy for WECs, for a flap-type device. The main components of this theory are discussed, while highlighting its appealing characteristics for this energy-maximising application. In addition, numerical results are presented for both monochromatic and polychromatic wave inputs.

© 2018, IFAC (International Federation of Automatic Control) Hosting by Elsevier Ltd. All rights reserved.

Keywords: Optimal Control, Wave Energy Converter, Moment Domain, Energy Maximisation

1. INTRODUCTION

Energy from ocean waves has the potential to fulfill the worldwide energy demand, with an estimation of 32.000 TWh/year (Mork et al., 2010). This motivates researchers to obtain a better understanding of the underlying issues behind harvesting wave energy. As a result, one of the most consistent outcomes (see, for example, (Ringwood et al., 2014)) is that Wave Energy Converters (WECs) require an optimised process that ensures a maximum energy absorption from waves, while respecting the physical limitations of both the device and the Power Take-Off (PTO) system. Such an optimisation procedure can be formulated as an optimal control problem.

Several strategies have been proposed to formulate and solve this energy-maximising control objective. Among these strategies, Model Predictive Control (MPC) is currently one of the most adopted formulations in the wave energy community. Nevertheless, the computational burden behind MPC can render the controller unsuitable for real-time applications (Faedo et al., 2017). Alternative strategies, such as spectral and pseudospectral methods (see (Faedo et al., 2017)), have recently emerged as an attempt to overcome the potentially demanding computational effort behind MPC. Computing this energy-maximising control law in real-time remains a challenge among the wave energy research community, and most of the proposed real-time strategies are usually inherently suboptimal.

Recently, the foundations of a novel formulation based on current advances in model order reduction by moment-matching (see, for example, (Astolfi, 2010)) has been developed in (Faedo et al., 2018). This strategy exploits the steady-state response of the WEC, providing a suitable set of mappings to compute an energy-maximising optimal control law in real-time. From now on, we refer to the framework induced by moment-matching as the moment-domain formulation of a system. This paper presents the application of this moment-based optimal control strategy to design an energy-maximising controller for a flap-type WEC, subject to constraints on the oscillation amplitude, velocity and actuator (PTO) input.

1.1 Notation and Preliminaries

Standard notation is considered through this study, with some exceptions further detailed in this preliminary section. $\mathbb{R}^+$ ($\mathbb{R}^-$) denotes the set of non-negative (non-positive) real numbers. $\mathbb{C}^0$ denotes the set of pure-imaginary complex numbers and $\mathbb{C}^-$ denotes the set of complex numbers with negative real part. The symbol 0 stands for any zero element, according to the context. The symbol $\mathbb{I}_n$ denotes an order n identity matrix, while the notation $\mathbf{1}_{n\times m}$ is used to denote a $n \times m$ Hadamard identity matrix (i.e. a $n \times m$ matrix with all its entries equal to 1). The spectrum of a matrix $A \in \mathbb{R}^{n\times n}$, i.e. the set of its eigenvalues, is denoted as $\sigma(A)$. The symbol $\bigoplus$ denotes the direct sum of n matrices, i.e. $\bigoplus_{i=1}^{n} A_i = \text{diag}(A_1, A_2, \ldots, A_n)$. The *Kronecker product* between two matrices $M_1 \in \mathbb{R}^{n\times m}$ and $M_2 \in \mathbb{R}^{p\times q}$ is denoted as $M_1 \otimes M_2 \in \mathbb{R}^{np\times mq}$. The convolution between two functions $f(t)$ and $g(t)$ over a finite range $[0, t]$, i.e. $\int_0^t f(\tau)g(t-\tau)d\tau$ is denoted as $f * g$. Finally, the symbol $\varepsilon_n \in \mathbb{R}^{n\times 1}$ denotes a vector with odd components equal to 1 and even components equal to 0.

In the remainder of this section the formal definition of the *Kronecker sum* is provided, since its definition in the literature can be often ambiguous.

⋆ This material is based upon works supported by Science Foundation Ireland under Grant no. 13/IA/1886.

2405-8963 © 2018, IFAC (International Federation of Automatic Control) Hosting by Elsevier Ltd. All rights reserved.
Peer review under responsibility of International Federation of Automatic Control.
10.1016/j.ifacol.2018.09.468

Definition 1. (Brewer, 1978) The *Kronecker sum* between two matrices P_1 and P_2, with $P_1 \in \mathbb{R}^{n\times n}$ and $P_2 \in \mathbb{R}^{k\times k}$, is defined (and denoted) as

$$P_1 \hat{\oplus} P_2 \triangleq P_1 \otimes \mathbb{I}_k + \mathbb{I}_n \otimes P_2. \tag{1}$$

2. MOMENT-BASED DESCRIPTION OF A SYSTEM

The moment-based formulation, as considered in this study, was first formulated in (Astolfi, 2010), with the purpose of developing reduced-order models for linear and non-linear dynamical systems. This mathematical foundation is extrapolated to the analysis of the steady-state behaviour of dynamical systems in (Scarciotti and Astolfi, 2016). A brief summary of the key elements of this moment-based theory is presented in the following.

2.1 Moments for Linear Systems

In this subsection, the notion of *moment* for linear systems, as formulated in (Astolfi, 2010), is recalled. Consider a finite-dimensional, single-input, single-output, continuous-time system described, for $t \geq 0$, by the state-space model

$$\begin{aligned} \dot{x}(t) &= Ax(t) + Bu(t), \\ y(t) &= Cx(t), \end{aligned} \tag{2}$$

where $x(t) \in \mathbb{R}^n$, $u(t) \in \mathbb{R}$, $y(t) \in \mathbb{R}$, $A \in \mathbb{R}^{n\times n}$, $B \in \mathbb{R}^{n\times 1}$ and $C \in \mathbb{R}^{1\times n}$. Consider the associated transfer function

$$H(s) = C(s\mathbb{I}_n - A)^{-1}B \tag{3}$$

and assume that (2) is controllable and observable.

Definition 2. (Antoulas, 2005) The 0-moment of system (2) at $s_i \in \mathbb{C}$ is the complex number $\eta_0(s_i) = C\left(s_i\mathbb{I}_n - A\right)^{-1}B$. The k-moment of system (2) at $s_i \in \mathbb{C}$ is the complex number

$$\eta_k(s_i) = \frac{(-1)^k}{k!}\left[\frac{d^k}{ds^k}\left(C(s\mathbb{I}_n - A)^{-1}B\right)\right]_{s=s_i}, \tag{4}$$

with $k \geq 1$ integer.

In (Astolfi, 2010), it is shown that the moments of system (2) are in a one-to-one relation with the steady-state response (provided it exists) of the output of the interconnection between a signal generator and system (2). This result is recalled, without proof, in the following theorem (the reader is referred to (Astolfi, 2010; Scarciotti and Astolfi, 2017b) for a comprehensive proof).

Theorem 1. (Astolfi, 2010; Scarciotti and Astolfi, 2017b,a) Consider system (2) and the signal generator

$$\begin{aligned} \dot{\xi}(t) &= S\,\xi(t), \\ u(t) &= L\,\xi(t), \end{aligned} \tag{5}$$

with $\xi(t) \in \mathbb{R}^{\nu\times 1}$, $S \in \mathbb{R}^{\nu\times\nu}$, $L \in \mathbb{R}^{1\times\nu}$ and $\xi(0) \in \mathbb{R}^{\nu\times 1}$. Assume that the triple $(L, S, \xi(0))$ is minimal, $\sigma(A) \subset \mathbb{C}^-$, $\sigma(S) \subset \mathbb{C}^0$ and the eigenvalues of S are simple. Let $\Pi \in \mathbb{R}^{n\times\nu}$ be the (unique) solution of the Sylvester equation

$$A\Pi + BL = \Pi S. \tag{6}$$

Then, there exists a one-to-one relation between the moments $\eta_0(s_1)$, $\eta_0(s_2)$, …, $\eta_0(s_\nu)$, with $s_i \in \sigma(S)$ for all $i = 1, \ldots, \nu$, and the steady-state response $C\Pi\xi$ of the output y of the interconnection of system (2) with the signal generator (5) (as in Figure 1). In fact, the moments are uniquely determined by the matrix $C\Pi$.

Moreover, system (2) has a global invariant manifold described by $\mathscr{M} = \{(x, \xi) \in \mathbb{R}^{n+\nu\times 1} : x = \Pi\xi\}$. Hence, the expression, $\forall t \geq 0$,

$$x(t) = \Pi\xi(t) + e^{At}(x(0) - \Pi\xi(0)), \tag{7}$$

holds.

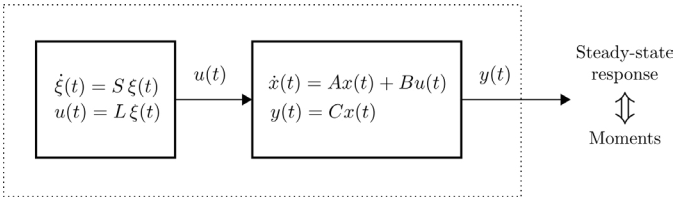

Figure 1. Schematic of the interconnection between the system (2) and the signal generator (5) (adapted from (Astolfi, 2010)).

As discussed in (Scarciotti and Astolfi, 2017a), the assumption on the eigenvalues of S is a sensible hypothesis, since any contribution from a stable mode will decay exponentially to zero. The minimality of the triple $(L, S, \xi(0))$ implies the observability of (L, S) and the controllability of $(S, \xi(0))$.

Remark 1. Note that the steady-state output y_{ss} of the interconnected system in Figure 1 can be computed from (7) as $y_{ss}(t) = C\Pi e^{St}\xi(0)$.

Definition 3. We call the matrix $C\Pi \equiv \bar{Y}$ the *moment-domain equivalent* of $y(t)$.

3. WEC CONTROL PROBLEM FORMULATION

In this study, a flap-type WEC is considered, hinged on one axis, as illustrated in Figure 2. This flap device is considered in (Giorgi and Ringwood, 2018) and is hinged at a depth $h = 13$[m], with a thickness $D = 2$[m] and width $W = 26$[m]. Applying Euler's second law of motion to the flap-type device, the following linear hydrodynamic formulation is obtained:

$$m\ddot{x}(t) = \mathcal{F}_r(t) + \mathcal{F}_h(t) + \mathcal{F}_{exc}(t) + u(t), \tag{8}$$

where m is the moment of inertia of the body with respect to the hinged axis, $x(t)$ the oscillation amplitude, $\mathcal{F}_{exc}(t)$ the wave excitation torque , $\mathcal{F}_r(t)$ the radiation torque, $\mathcal{F}_h(t)$ the hydrostatic restoring torque, and $u(t)$ is the control input applied through the PTO system. The hydrostatic torque can be linearly approximated as $-s_h x(t)$ where $s_h > 0$ is the hydrostatic restoring coefficient. The radiation torque $\mathcal{F}_r(t)$ is also modelled based on linear potential theory and, using the well-known Cummins' equation (Cummins, 1962), is

$$\mathcal{F}_r(t) = -m_\infty\ddot{x}(t) - \int_0^{+\infty}\zeta(\tau)\dot{x}(t-\tau)d\tau, \tag{9}$$

where $m_\infty > 0$ represents the added-inertia at infinite frequency and $\zeta(t)$ is the (causal) radiation impulse response. Finally, the linearized equation of motion of the WEC is given by

$$(m+m_\infty)\ddot{x}(t) + \zeta(t) * \dot{x}(t) + s_h x(t) = \mathcal{F}_{exc}(t) - u(t), \tag{10}$$

The equation of motion (10) is of a Volterra integro-differential form, specifically of the convolution class. The internal stability of such an equation, for the WEC case, has been analysed and guaranteed for any physically meaningful values of the parameters and the convolution kernel $\zeta(t)$ involved (Falnes, 2002).

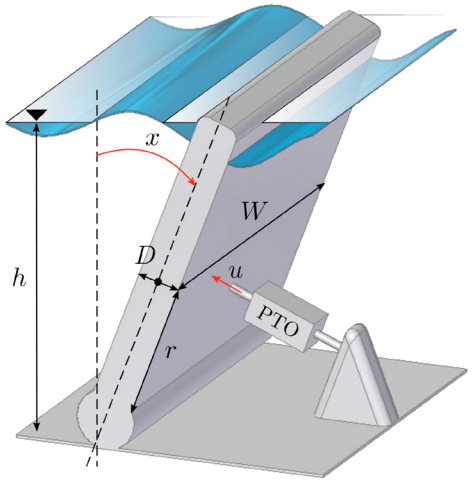

Figure 2. Flap-type wave energy converter

3.1 Path Constraints

As stated in Section 1, any approach to an optimal control solution for WECs must consider the physical limitations constraining the body's motion and the PTO characteristics.

Constraints are often considered, for the WEC control problem formulation, on the amplitude (displacement) $x(t)$, velocity $\dot{x}(t)$ and on the control input (PTO force) $u(t)$, which can be written in a compact form as

$$\begin{cases} |x(t)| \leq X_{max}, \\ |\dot{x}(t)| \leq V_{max} \\ |u(t)| \leq U_{max}, \end{cases} \quad \forall t \in \mathbb{R}, (X_{max}, V_{max}, U_{max}) \in \mathbb{R}^{+^3}. \tag{11}$$

3.2 Optimal Control Formulation

The main objective of a wave energy device is harvesting energy from the incoming wave field, in which the device is immersed. Therefore, the optimal control objective is to maximise the absorbed energy over the time interval $[t, t+T]$, given by

$$\mathcal{J} = \int_t^{t+T} u(\tau)\dot{x}(\tau)\, d\tau, \tag{12}$$

while respecting the path constraints defined in (11). Consequently, the optimal control objective can be formulated as,

$$\max_{u(t)} \ \mathcal{J} \quad \text{subject to} \begin{cases} \text{system dynamics (10)}, \\ \text{path constraints (11)}. \end{cases} \tag{13}$$

To maximise the absorbed energy, as stated in (13), future knowledge of the excitation force is required, which only becomes trivial in the case in which the input $\mathcal{F}_{exc}(t)$ is monochromatic, i.e. it can be represented by $\mathcal{F}_{exc}(t) = F\cos(\omega_0 t)$. This is no longer true in a realistic sea case, in which the excitation force is polychromatic, i.e. it is composed of several harmonics of a fundamental frequency ω_0, and prediction of the future values of $\mathcal{F}_{exc}(t)$ is required within this energy-maximising objective framework. The optimal control formulation stated in (13) has been solved using different strategies, including diverse modifications on the system dynamics considered, objective function, optimisation method and optimisation algorithms involved (Faedo et al., 2017).

4. MOMENT-BASED WEC CONTROL FORMULATION

In this section, the moment-based theory is considered for the WEC energy-maximising optimal control formulation described in (13). Since the moment-domain theory for linear systems is based on a state-space representation, the WEC dynamics given in (10) are re-written in a more suitable structure, namely

$$\dot{\varphi}(t) = A_\varphi \varphi(t) + B_\varphi \mathscr{U}(t), \quad y_\varphi(t) = C_\varphi \varphi(t), \tag{14}$$

where $\varphi(t) = [x(t),\, \dot{x}(t)]^\intercal \in \mathbb{R}^{n\times 1}$, with $n = 2$, is the state-vector of the continuous-time model and $y_\varphi(t) = \dot{x}(t) \in \mathbb{R}$ is the output of the system. The function $\mathscr{U}(t)$, assumed to be the input of system (14), is defined as

$$\mathscr{U}(t) = \mathcal{F}_{exc}(t) - u(t) - \zeta(t) * \dot{x}(t), \tag{15}$$

where the actual physical inputs are the excitation torque $F_{exc}(t)$ and the control law $u(t)$. The radiation torque convolution term is included as a feedback term, being a pure algebraic manipulation to develop a state-space representation of (10). Under this assumption, the matrices in (14) are given by

$$A_\varphi = \begin{bmatrix} 0 & 1 \\ -\dfrac{s_h}{m+\mu_\infty} & 0 \end{bmatrix}, \; B_\varphi = \begin{bmatrix} 0 \\ \dfrac{1}{m+\mu_\infty} \end{bmatrix}, \; C_\varphi = [0 \;\; 1]\,. \tag{16}$$

Following the moment-based theory, both inputs of (14), $\mathcal{F}_{exc}(t)$ and $u(t)$, are represented by signal generators, written in implicit form as

$$\begin{aligned} \dot{\xi}_{exc}(t) &= S\,\xi_{exc}(t), & \dot{\xi}_u(t) &= S\,\xi_u(t), \\ \mathcal{F}_{exc}(t) &= L_{exc}\,\xi_{exc}(t), & u(t) &= L_u\,\xi_u(t), \end{aligned} \tag{17}$$

where $\xi_{exc}(t) \in \mathbb{R}^{\nu\times 1}$, $\xi_u(t) \in \mathbb{R}^{\nu\times 1}$, with $\xi_{exc}(0) \neq 0$, $\xi_u(0) \neq 0$ and $S \in \mathbb{R}^{\nu\times\nu}$. The pairs (S, L_{exc}) and (S, L_u) are assumed to be observable, with $L_u \in \mathbb{R}^{1\times\nu}$ and $L_{exc} \in \mathbb{R}^{1\times\nu}$. Note that L_u and L_{exc} are the moment-domain equivalents of the control input and the excitation torque, respectively. Furthermore, without loss of generality, it is assumed that $\xi_u(0) = \xi_{exc}(0) = \xi(0) = \varepsilon_\nu$. The matrix S in (17), can be written in a simple block-diagonal form as

$$S = \bigoplus_{p=1}^{k} \begin{bmatrix} 0 & \omega_p \\ -\omega_p & 0 \end{bmatrix}, \tag{18}$$

where $\nu = 2k$. Then, the steady-state response $y_{\varphi_{ss}}(t)$ of system (14) driven by the sum of the outputs of both signal generators in (17) can be computed using a Sylvester equation (see Remark 1). Considering superposition, the resulting Sylvester equation for the WEC device case is given by

$$A_\varphi \Pi_\varphi + B_\varphi(L_{exc} - L_u - \bar{R}) = \Pi_\varphi S, \tag{19}$$

where $\Pi_\varphi \in \mathbb{R}^{n\times\nu}$ and $\bar{R}$ is the moment-domain representation of the radiation convolution term, which is discussed later in this section. Note that the moment-domain equivalent of the velocity can be simply expressed in terms of the solution of (19) as $\bar{V} = C_\varphi \Pi_\varphi$.

Proposition 1. (Faedo et al., 2018) The moment-domain equivalent of the convolution integral in (9) can be computed as

$$\bar{R} = \bar{V}\mathscr{R}, \tag{20}$$

where $\mathscr{R} \in \mathbb{R}^{\nu\times\nu}$ is a block-diagonal matrix defined by

$$\mathscr{R} = \bigoplus_{p=1}^{f} \begin{bmatrix} r_{\omega_p} & -m_{\omega_p} \\ m_{\omega_p} & r_{\omega_p} \end{bmatrix}, \tag{21}$$

and its entries depend on the radiation added-mass $A(\omega)$ and radiation damping $B(\omega)$ of the device at each specific frequency induced by the eigenvalues of S (the reader is referred to (Falnes, 2002) for a comprehensive definition of $A(\omega)$ and $B(\omega)$), as

$$r_{\omega_p} = B(\omega_p), \quad m_{\omega_p} = -\omega_p\left[A(\omega_p) - \mu_\infty\right]. \tag{22}$$

With the analytical definition of the moment-domain equivalent of the radiation torque convolution term, the following proposition is recalled from (Faedo et al., 2018), which facilitates the solution of (19).

Proposition 2. (Faedo et al., 2018) The moment-domain equivalent of the output y_φ of system (14) can be computed as

$$\bar{V} = (L_{exc} - L_u)\Phi_\varphi^{\mathscr{R}}, \tag{23}$$

where

$$\begin{aligned} \Phi_\varphi^{\mathscr{R}} &= \left[\left(\mathbb{I}_\nu + \Phi_\varphi \mathscr{R}^\intercal\right)^{-1}\Phi_\varphi\right]^\intercal, \\ \Phi_\varphi &= (\mathbb{I}_\nu \otimes C_\varphi)\left(S \hat{\oplus} A_\varphi\right)^{-1}(\mathbb{I}_\nu \otimes -B_\varphi), \end{aligned} \tag{24}$$

with $\Phi_\varphi^{\mathscr{R}} \in \mathbb{R}^{\nu\times\nu}$ and $\Phi_\varphi \in \mathbb{R}^{n\nu\times n\nu}$.

The objective function (13) depends explicitly on the average power absorbed by the PTO system over a time interval $[t, t+T]$, where T is now defined as $T = 2\pi/\omega_0$, and denotes the *fundamental period*. Likewise, ω_0 represents the *fundamental frequency*. This is consistent with the assumption for the numerical representation of the wave excitation force: $\mathcal{F}_{exc}(t)$ can be expressed as the sum of k harmonics of the fundamental frequency ω_0 (Mérigaud and Ringwood, 2018). The following proposition allows the optimal control objective $\mathcal{J}$ (13) to be written in the moment-domain.

Proposition 3. (Faedo et al., 2018) Define the constant values of S in (18) as $\omega_p = p\,\omega_0, \forall\, p = 1, \ldots, k$ with $k \geq 1$ integer (i.e. k harmonics of the fundamental frequency ω_0). Then, the energy-maximising optimal control formulation over the time period $[t, t+T]$, where $T = 2\pi/\omega_0$, can be written in the moment-domain as

$$\max_{L_u} \ \frac{1}{2}\bar{V}L_u^\intercal. \tag{25}$$

Substituting $\bar{V}$ (23) into the optimal control formulation (25), the energy-maximising controller can be designed by maximising the absorbed energy as

$$\max_{L_u} \ -\frac{1}{2}L_u\Phi_\varphi^{\mathscr{R}}L_u^\intercal + \frac{1}{2}L_{exc}\Phi_\varphi^{\mathscr{R}}L_u^\intercal, \tag{26}$$

which represents a quadratic program (QP) involving only L_u. The mixed state-input formulation (25) has been transformed into an unconstrained quadratic program.

In the following, an important result regarding the concavity of the quadratic program involved in the moment-domain control formulation, defined in (26), is recalled.

Proposition 4. (Faedo et al., 2018) The QP formulation in (26) is strictly concave for any physically meaningful values of the system parameters in (16).

Remark 2. Proposition 4 implies that the unconstrained moment-domain optimal control formulation for the WEC device (26) always has a unique (global) maximum, allowing the utilisation of well-known and efficient quadratic programming solvers (Boyd and Vandenberghe, 2004) to compute the optimal control law in real-time.

4.1 Force, Velocity and Amplitude constraints

As discussed in Section 3.1, constraints on the control input, the oscillation amplitude and velocity, reflect physical limitations on the device. These constraints can be considered in the moment-domain framework as follows. Recall (11) and, using the result on moment-based theory stated in Remark 2, the following mappings

$$\begin{cases} |u(t)| \leq U_{max}, \\ |u(t)| \leq V_{max}, \\ |x(t)| \leq X_{max}, \end{cases} \quad \mapsto \quad \begin{cases} |L_u\, e^{St}\varepsilon_\nu| \leq U_{max}, \\ |\bar{V}\, e^{St}\varepsilon_\nu| \ \leq V_{max}, \\ |\bar{X}\, e^{St}\varepsilon_\nu| \ \leq X_{max}, \end{cases} \tag{27}$$

where $\bar{X}$ represents the moment-domain equivalent of the amplitude $x(t)$, hold.

One possible approach to deal with the constraints defined in (27) is to enforce them only at a set of specified time instants (collocation points), i.e. $t_1, \ldots, t_{N_c}$. Define the vectors $\Lambda \in \mathbb{R}^{\nu\times N_c}$ and $\Delta \in \mathbb{R}^{\nu\times 2N_c}$ as

$$\Lambda = \left[e^{S\,t_0}\varepsilon_\nu \ \ldots \ e^{S\,t_{N_c}}\varepsilon_\nu\right], \quad \Delta = \left[\Lambda \ -\Lambda\right]. \tag{28}$$

Then, the following proposition is recalled from (Faedo et al., 2018).

Proposition 5. (Faedo et al., 2018) The constraint mappings defined in (27), evaluated at the collocation points, can be written as a set of linear inequalities given by

$$\begin{aligned} &L_u\Delta \leq U_{max}\mathbf{1}_{1\times 2N_c}, \\ &L_u(-\Phi_\varphi^{\mathscr{R}})\Delta \leq V_{max}\mathbf{1}_{1\times 2N_c} - L_{exc}\Phi_\varphi^{\mathscr{R}}\Delta, \\ &L_u(-\Phi_\varphi^{\mathscr{R}})S^{-1}\Delta \leq X_{max}\mathbf{1}_{1\times 2N_c} - L_{exc}\Phi_\varphi^{\mathscr{R}}S^{-1}\Delta. \end{aligned} \tag{29}$$

Finally, the inequality constrained QP optimal control formulation can be written as

$$\begin{aligned} &\max_{L_u} \ -\frac{1}{2}L_u\Gamma_*^{\mathscr{R}}L_u^\intercal + \frac{1}{2}L_{exc}\Gamma_*^{\mathscr{R}}L_u^\intercal, \\ &\text{subject to:} \\ &L_u\Delta \leq U_{max}\mathbf{1}_{1\times 2N_c}, \\ &L_u(-\Phi_\varphi^{\mathscr{R}})\Delta \leq V_{max}\mathbf{1}_{1\times 2N_c} - L_{exc}\Phi_\varphi^{\mathscr{R}}\Delta, \\ &L_u(-\Phi_\varphi^{\mathscr{R}})S^{-1}\Delta \leq X_{max}\mathbf{1}_{1\times 2N_c} - L_{exc}\Phi_\varphi^{\mathscr{R}}S^{-1}\Delta. \end{aligned} \tag{30}$$

where the uniqueness of the global maximum, for the unconstrained case, is guaranteed by Proposition 4.

5. NUMERICAL RESULTS

In this section, a flap-type WEC device is considered to illustrate the effectiveness of the proposed strategy. The hydrodynamic coefficients that characterise this device (added-mass and radiation damping) can be appreciated in Figure 3 . Simulations of the control strategy are given both for regular and irregular waves scenarios.

When regular waves are considered, all the numerical results observe a wave period of 10 seconds and a wave

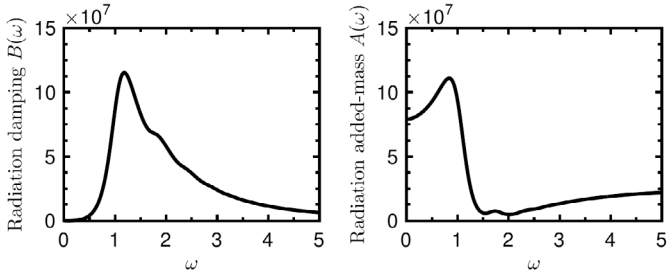

Figure 3. WEC hydrodynamic coefficients $B(\omega)$ and $A(\omega)$.

height of 5 metres. Two separate simulation scenarios are considered. The first scenario is a partially constrained optimal control case, where the oscillation amplitude $x(t)$ and velocity $\dot{x}(t)$ of the device are constrained, with maximum allowed values given by $X_{max} = 45$ [deg] and $V_{max} = 30$ [deg/s] (performance denoted in the subsequent figures with a dotted-black line), respectively. In the second scenario, an additional constraint is considered for the control torque $u(t)$, set to a value of $U_{max} = 2.5 \times 10^7$ [Nm] (performance denoted in the subsequent figures with a solid-green line). Before going further with this numerical example, a simple analysis is performed to select an appropriate number of frequency components (harmonics) to represent the control input $u(t)$, which can be done by taking into account the trade-off between computational time, smoothness of the control signal and final energy absorption (the reader is referred to (Faedo et al., 2018) for further details on this trade-off). The smoothness of $u(t)$ is not discussed in this paper due to space restriction. Figure 4 depicts the ratio of absorbed energy computed as $R_f = E_k/E_{50}$, where E_k is the final absorbed energy obtained when considering k frequency components to describe $u(t)$. The value E_{50} is considered as the maximum energy achievable, since almost an imperceptible improvement can be obtained when considering more than 50 components.

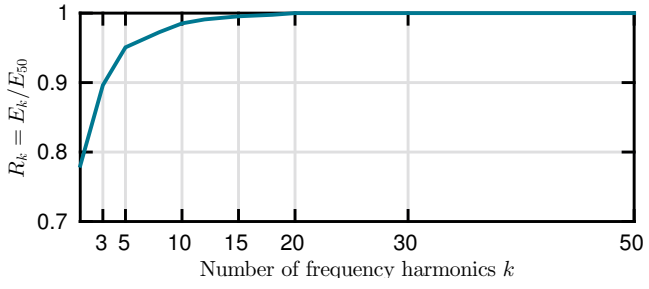

Figure 4. Ratio of absorbed energy R_k as a function of the number of frequency harmonics k

Although all the computations performed for this case study can be successfully done in real-time (implemented in MATLAB), it can be appreciated in Figure 4 that, when selecting more than approximately 10 frequency components, the absorption ratio R_k is almost one, suggesting that 10 harmonics can reasonably describe the optimal control input, avoiding an unnecessary increase in the problem complexity.

Figure 5 depicts simulation results for a regular wave input, for both optimal control scenarios. It can be appreciated that, in the case where only only the amplitude and velocity are constrained to X_{max} and V_{max}, the control input consistently violates the proposed maximum limit for the PTO force U_{max}. This is subsequently solved by adding the PTO constraint to the moment-domain optimisation computation, as is evident from Figure 5, where all the variables are confined between the specified maximum absolute values.

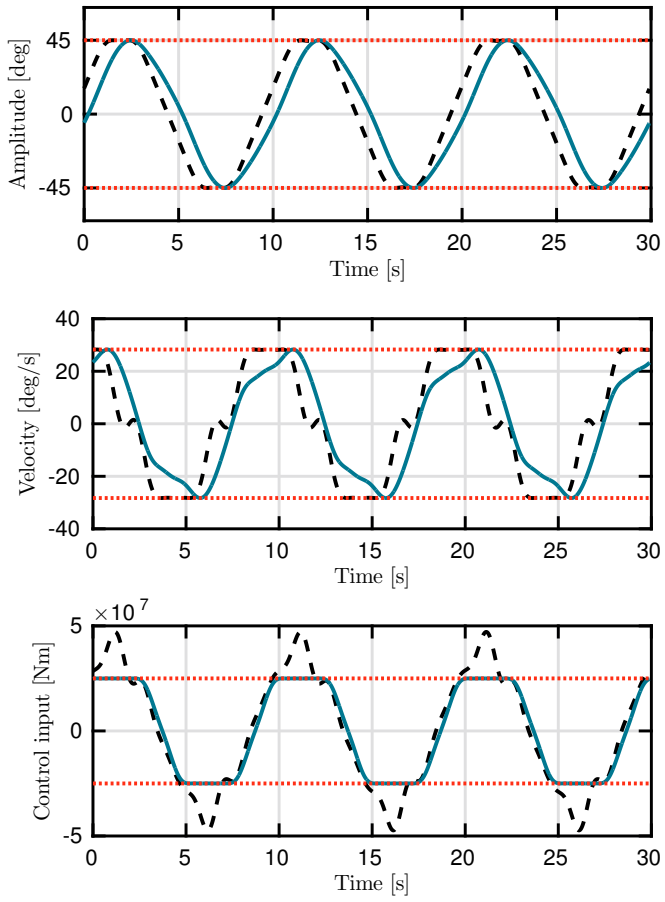

Figure 5. Simulation results for a regular wave input (period 10[s] and height 5[m]), for both optimal control scenarios: constraints considered in amplitude and velocity (dotted-black) and (in addition) on the control input (solid-green).

For the polychromatic input case, the irregular waves are generated from a JONSWAP spectrum (Hasselmann, 1973) shown in Figure 6 (peak period $T_p = 10$[s], significant wave height $H_s = 5$[m], peak enhancement factor $\gamma = 3.3$). Figure 7 illustrates the application case with the polychromatic input. In this scenario, and using a similar analysis as in the regular waves case, the value of k is set to 30. As in the monochromatic input situation, it can be acknowledged that all the variables can be successfully restricted to the desired maximum values, while optimising the final energy absorption.

6. CONCLUSION

In this paper, a recently developed moment-domain based formulation is considered to design an energy-maximising controller for a flap-type WEC. The resulting optimal con-

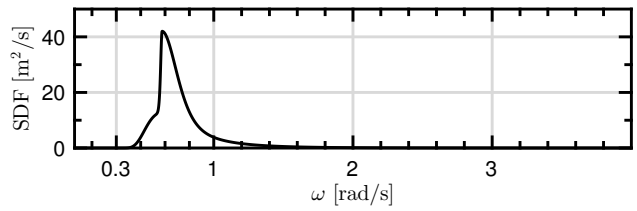

Figure 6. JONSWAP spectrum (peak period $T_p = 10$[s], significant wave height $H_s = 5$[m], peak enhancement factor $\gamma = 3.3$)

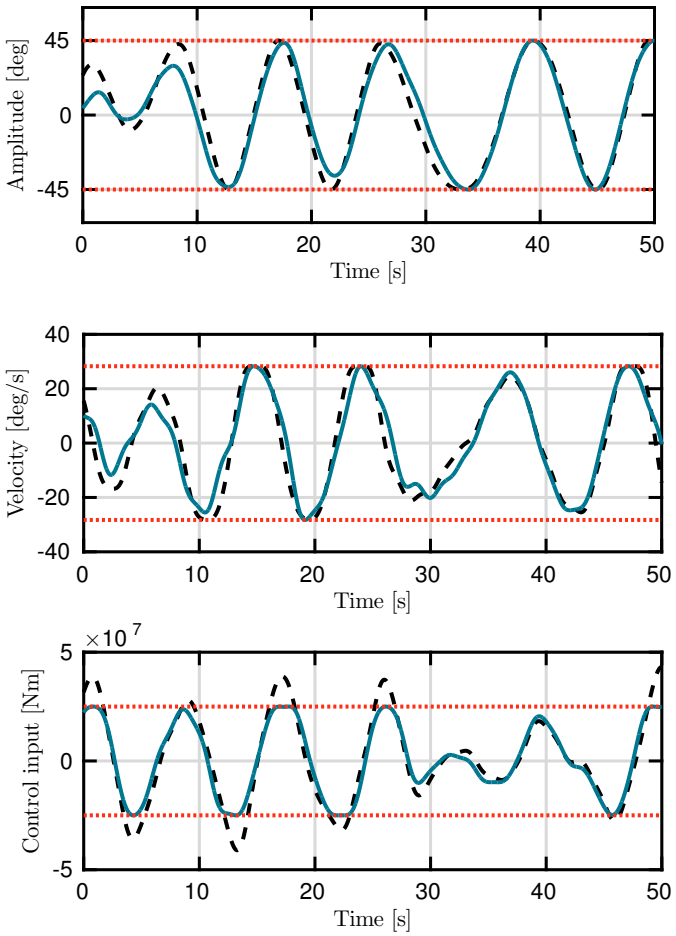

Figure 7. Simulation results for an irregular wave input (peak period 5[s] and significant wave height 5[m]), for both optimal control scenarios: constraints considered in amplitude and velocity (dotted-black) and (in addition) on the control input (solid-green).

trol problem is a concave quadratic program, allowing the real-time computation of the optimal control input, based on the availability of extremely efficient solvers that can be used within such an optimisation scheme. Moreover, this mathematical formulation observes physical constraints by a suitable mapping based on moment-theory. The strategy is tested under regular and irregular waves excitation, considering constraints in both the oscillation amplitude and velocity of the device, and the PTO control torque.

ACKNOWLEDGEMENTS

The authors are sincerely grateful to Prof. Alessandro Astolfi and Dr. Giordano Scarciotti from Imperial College London, for useful discussions on the moment-based theory. This material is based upon works supported by Science Foundation Ireland under Grant no. 13/IA/1886.

REFERENCES

Antoulas, A.C. (2005). *Approximation of large-scale dynamical systems*, volume 6. SIAM.

Astolfi, A. (2010). Model reduction by moment matching for linear and nonlinear systems. *IEEE Transactions on Automatic Control*, 55(10), 2321–2336.

Boyd, S. and Vandenberghe, L. (2004). *Convex Optimization*. Cambridge University Press.

Brewer, J. (1978). Kronecker products and matrix calculus in system theory. *IEEE Transactions on Circuits and Systems*, 25(9), 772–781.

Cummins, W. (1962). The impulse response function and ship motions. Technical report, DTIC Document.

Faedo, N., Olaya, S., and Ringwood, J.V. (2017). Optimal control, mpc and mpc-like algorithms for wave energy systems: An overview. *IFAC Journal of Systems and Control*, 1, 37–56.

Faedo, N., Scarciotti, G., Astolfi, A., and Ringwood, J.V. (2018). Energy-maximising control of wave energy converters using a moment-domain representation. *Control Engineering Practice (under review)*.

Falnes, J. (2002). *Ocean Waves and Oscillating Systems: Linear Interactions Including Wave-Energy Extraction*. Cambridge University Press.

Giorgi, G. and Ringwood, J.V. (2018). Comparing nonlinear hydrodynamic forces in heaving point absorbers and oscillating wave surge converters. *Journal of Ocean Engineering and Marine Energy*, 4(1), 25–35.

Hasselmann, K. (1973). Measurements of wind wave growth and swell decay during the Joint North Sea Wave Project (JONSWAP). *Dtsch. Hydrogr. Z.*, 8, 95.

Mérigaud, A. and Ringwood, J.V. (2018). Free-surface time-series generation for wave energy applications. *IEEE Journal of Oceanic Engineering*, 43(1), 19–35.

Mork, G., Barstow, S., Kabuth, A., and Pontes, M.T. (2010). Assessing the global wave energy potential. In *ASME 2010 29th International Conference on Ocean, Offshore and Arctic Engineering*, 447–454.

Ringwood, J.V., Bacelli, G., and Fusco, F. (2014). Energy-maximizing control of wave-energy converters: The development of control system technology to optimize their operation. *IEEE Control Systems*, 34(5), 30–55.

Scarciotti, G. and Astolfi, A. (2016). Moment-based discontinuous phasor transform and its application to the steady-state analysis of inverters and wireless power transfer systems. *IEEE Transactions on Power Electronics*, 31(12), 8448–8460.

Scarciotti, G. and Astolfi, A. (2017a). Data-driven model reduction by moment matching for linear and nonlinear systems. *Automatica*, 79, 340–351.

Scarciotti, G. and Astolfi, A. (2017b). Nonlinear model reduction by moment matching. *Foundations and Trends in Systems and Control*, 4(3-4), 224–409.